

USING ADVANCED IMAGING TO STUDY FISH

A Thesis

by

ZOE SWEZY BROWNING

Submitted to the Office of Graduate Studies of  
Texas A&M University  
in partial fulfillment of the requirements for the degree of

MASTER OF SCIENCE

Chair of Committee, Duncan MacKenzie  
Co-Chair of Committee, Ann Kier  
Committee Member, Mark Lenox  
Head of Department, Linda Logan

August 2013

Major Subject: Biomedical Sciences

Copyright 2013 Zoe Swezy Browning

## ABSTRACT

Although mammals are the most commonly utilized laboratory animal, laboratory animal medicine continually seeks to replace them with animals of lower phylogenetic classification. Fish are becoming increasingly important as investigators seek alternative animal models for research. Fish can provide an economical and feasible alternative to typical mammalian models; moreover, many fish, which have comparatively short life spans, can easily reproduce in the laboratory. One key area of animal health research in which fish have been underutilized is the field of advanced imaging. Although many images of fish have been captured through the use of computed tomography (CT), radiography, and ultrasonography, these images have been primarily utilized for anatomical study. In addition, fish have never before been studied with positron emission tomography/ computed tomography (PET/CT). My objectives were to determine if these imaging techniques can be used to obtain physiological information from fish, therefore making it more likely that fish can be utilized as replacement animals using these new imaging techniques (CT, PET/CT). I performed two different types of studies to assess the potential application of advanced imaging techniques to fish. In the first experiment, microCT was used to characterize otolith deformity in vitamin C deficient captive-raised red drum and relate the deformity to behavioral and physiological changes. I found that the normal and abnormal fish had statistically significant differences in behavior, cortisol levels, and otolith volume and density. MicroCT assessment of abnormal fish revealed operculum abnormalities, malocclusions,

and several types of otolith malformations. Therefore, the affected fish had not only an abnormal skeletal appearance but also significantly abnormal behavior and cortisol responses. In the second experiment, fluorodeoxyglucose-positron emission tomography/computed tomography (FDG-PET/CT) was used to quantify glucose uptake in select organs prior to carcinogenesis studies in fish. The quantified glucose uptake was compared to published data on humans, mice, and dogs. Rapid, quantifiable glucose uptake was demonstrated, particularly in brain, kidneys, and liver in all imaged fish species. Glucose uptake in the major organ systems of fish was closer to that in humans than uptake in mice or dogs, indicating that fish may serve as an effective alternative animal model for tumor studies using this technology. Other applications for this technique in fish may include metabolism studies and screening for environmental carcinogenesis. I found that both microCT and PET/CT imaging provided useful and meaningful results. In addition, the use of non-invasive scanning allows for re-use of fish, thus reducing the number of animal models used in experiments. These experiments suggest that fish will be good replacement models for mammals using these advanced imaging techniques.

## DEDICATION

To my husband, Joseph Browning, with whom nothing is impossible.

## ACKNOWLEDGEMENTS

I would like to thank my committee co-chairs, Dr. Ann Kier and Dr. Duncan MacKenzie, my committee member, Dr. Mark Lenox, and my resident director, Dr. Vince Gresham for their guidance and support throughout the course of this research.

I would like to thank Dr. Delbert Gatlin, Brian Ray, and Mark Webb for helping me procure fish. I would like to thank Dr. Ann Kier for providing funds for supplies. I would also like to thank Dr. Mark Lenox, Dr. Fred Clubb, Trevor Lancon, and Christine Pelham for their assistance with the imaging procedures. I gratefully acknowledge Dr. Christine Budke for her help with the statistics portion of this project. I would like to thank Dr. Duncan MacKenzie and Allison Wilkes for allowing me to collect data on the red drum in conjunction with their research, and Dr. Scott Jacques at Texas Veterinary Medical Diagnostic Laboratory for his help with the cortisol radioimmunoassay. I appreciate Julie Butler's help collecting the behavior data. I am grateful to Dr. Clay Ashley, Dr. James Elliott, Dr. Vincent Gresham, Dr. Ann Kier, Dr. Sara Lawhon, Dr. Duncan MacKenzie, and Allison Wilkes for reviewing earlier drafts of this manuscript. Thanks also go to my friends and colleagues and the comparative medicine department faculty and staff for making my time at Texas A&M University a great experience.

## NOMENCLATURE

AA	ascorbic acid
FDG	<sup>18</sup> F-fluorodeoxyglucose
PET	positron emission tomography
CT	computed tomography
ROI	region of interest
SUV	standard uptake value

## TABLE OF CONTENTS

	Page
ABSTRACT .....	ii
DEDICATION .....	iv
ACKNOWLEDGEMENTS .....	v
NOMENCLATURE.....	vi
TABLE OF CONTENTS .....	vii
LIST OF FIGURES.....	kx
LIST OF TABLES .....	x
CHAPTER I INTRODUCTION .....	1
CHAPTER II THE EFFECT OF OTOLITH MALFORMATION ON BEHAVIOR AND CORTISOL LEVELS IN JUVENILE RED DRUM FISH ( <i>Sciaenops ocellatus</i> ).....	6
Introduction .....	6
Materials and methods .....	8
Results.....	10
Discussion.....	11
CHAPTER III USING PET/CT IMAGING TO CHARACTERIZE 18 F- FLUORODEOXYGLUCOSE UTILIZATION IN FISH.....	15
Introduction.....	15
Materials and methods .....	18
Results.....	21
Discussion.....	23
CHAPTER IV SUMMARY AND CONCLUSIONS.....	27

REFERENCES .....	30
APPENDIX A.....	35



## LIST OF FIGURES

FIGURE		Page
1	Behavioral Comparison.....	36
2	Cortisol Comparison .....	37
3	MicroCT of Normal Drum .....	38
4	MicroCT of Abnormal Drum.....	39
5	MicroCT of Abnormal Drum Otoliths .....	40
6	Otolith Comparison.....	41
7	Tilapia FDG-PET/CT Image.....	42
8	Red Drum Group FDG-PET/CT Image.....	43
9	SUV in Each ROI Compared between Fish and Humans.....	44
10	SUV in Each ROI Compared between Fish, Dogs, Mice and Humans .....	45

## LIST OF TABLES

TABLE		Page
1	Behavioral Measurements .....	46
2	Summary of Differences between Normal and Abnormal Drum .....	47
3	Weight and Lengths of Fish.....	48
4	30 Minute SUV of Fish .....	50
5	60 Minute SUV of Fish .....	51

# CHAPTER I

## INTRODUCTION

The 3Rs, reduce, refine, and replace are the principle edicts of laboratory animal medicine.<sup>1</sup> Fish fulfill two of these edicts by providing good replacement animal models to reduce the use of mammalian species in research<sup>2</sup>. Fish are valuable as research models for a number of reasons, including portability, ease of laboratory culture, and short reproductive lifecycle. As a result, fish have been used for everything from prion research to genetic testing to cancer research<sup>3-8</sup>. They represent the largest and most diverse group of vertebrates and can easily be raised in the laboratory, often less expensively than other vertebrates<sup>9</sup>. Besides their importance as model systems for biological research, fish are useful economically and as a source of nutrition for humans. Aquatic biotechnology, aquaculture, is the fastest growing industry worldwide. Aquaculture production and the value of aquaculture products has doubled over the past ten years to become a multi-million dollar industry<sup>10</sup>. In addition to its obvious economic importance, aquaculture provides a critical portion of human nutrition due to the efficiency of feed conversion in fish<sup>11-13</sup>. Due to lower maintenance and respiratory costs, fish are more efficient converters of feed into meat than mammals. Worldwide, fish represent 6% of human dietary protein consumption. However, this percentage rises to as high as 22.3% in Asian countries<sup>10</sup>. Fish have also been extensively studied in carcinogenesis research. For instance, the novel fish neoplasia research of Mearl Stanton piqued the interest in the use of fish species for cancer research in 1965<sup>9</sup>. Since that time,

many fish species have been established as animal models for human neoplasms, notably rainbow trout with hepatocellular carcinomas<sup>9</sup>, platyfish/swordtails with melanomas<sup>14</sup>, catfish with epitheliomas<sup>15</sup>, and bicolor damselfish with schwannomas<sup>16</sup>. As early as the 1930s, zebrafish have been used as developmental and embryological model animal models of human disease<sup>3-8</sup>. There is one area of research, however, in which fish have been underutilized, the field of advanced imaging. Although many images of fish have been captured through the use of CT (computed tomography), radiographs, and ultrasound, these images have been primarily utilized for anatomical study. The primary goal of my research is to determine how fish can fit into current research involving advanced imaging's application to functional studies. By demonstrating how advanced imaging techniques for evaluating mammalian tumor growth and development are applicable to fish, I showed how fish may serve as highly useful adjuncts to traditional mammalian models while at the same time providing wholly unique approaches as replacement animals. As such, they may serve as useful new animal models for human carcinogenesis research. The novel aspects of my research are the first use of PET (positron emission tomography) imaging in fish and the use of CT imaging to reach functional conclusions by linking imaging data to fish behavior and physiology.

I explored two potential applications of advanced imaging techniques in fish. First, microCT and CT utilize tomography created by computer processing and digital geometry processing to generate a detailed anatomical three-dimensional image of the inside of an object from a large series of two-dimensional X-ray images taken around a

single axis of rotation<sup>17,18</sup>. This technique observes anatomic features of an organism in a three dimensional view.

I used this imaging technique in a novel way by linking internal deformities to physiologic and behavioral changes. In the first experiment, microCT was used to characterize otolith deformities captive-raised red drum (*Sciaenops ocellatus* L.) and relate deformity to behavior and physiology. Captive-raised red drum have been observed with phenotypic abnormalities, including deformities of the spine, jaw, and cephalic region, which were consistent with vitamin C deficiency during the larval stage. In light of their obvious skeletal abnormalities, I hypothesized that vitamin C deficient fish would have irregular otoliths that would alter behavior and stress response as compared with those of phenotypically normal fish. Cortisol was used to quantitate acute stress levels. Evaluation of behavior and cortisol levels was coupled with microCT assessment of normal and abnormal fish. The mean behavioral scores, cortisol levels, and otolith volume, mass, and density of normal and abnormal fish were analyzed by using the Student *t* test.

Another type of imaging, combined positron emission tomography/computed tomography (PET/CT), is a relatively new imaging modality that combines the functional images of PET with the anatomical information of CT. PET is capable of detecting areas of metabolic activity by using radio-labeled molecular probes with specific uptake rates<sup>19</sup>. The most commonly used PET tracer is 18 F-fluorodeoxyglucose (FDG), a glucose analogue that allows measurement and mapping of tissue glucose uptake<sup>20</sup>. FDG, like glucose, enters cells and is phosphorylated by hexokinase to FDG-6-

phosphate. Unlike glucose, FDG undergoes only the initial phosphorylation and is not further metabolized past F18-FDG-6-Phosphate and thus remains in the cell<sup>20,21</sup>. In normal tissues, FDG uptake peaks in the heart, liver, and kidneys shortly after administration<sup>22</sup>. In the presence of neoplasia, the tumor also takes up glucose/FDG rapidly, allowing for the visualization of the tumor mass *in vivo* over time<sup>17,23</sup>. The retention of the tracer is calculated as SUV (standard uptake value), the most widely used unit of measure of metabolic rate of glucose uptake<sup>18,22,23</sup>. SUVs provide highly reproducible parameters of cellular glucose metabolism, allowing for accurate comparison among PET studies<sup>23</sup>. However, the accuracy of PET measurements alone can be hampered by lack of sufficient anatomical detail. PET/CT imaging merges the two systems, combining the images acquired from both devices into one superimposed image. Thus, functional imaging obtained by PET can be more precisely correlated with anatomic three-dimensional imaging obtained by CT scanning. Post processing workstations allow for objective and subjective analysis of the imaging data.

In my second study, FDG-PET/CT was used to quantify glucose uptake in select organs of multiple fish species to establish baseline FDG values in fish. Fish were serially imaged at 30 and 60 minutes post injection of FDG. Based on mammalian studies and fish metabolism research, time contrast images provide the most accurate and sensitive information about fish glucose metabolism<sup>20,24</sup>. Post-acquisition, the FDG distribution of the entire imaging volume was analyzed in three dimensions using Siemens workstations. SUVs were computed for the following tissue volumes: heart, liver, intestines, brain, and muscle. Data obtained was analyzed by ANOVA, with a

$p < .05$  used for determining statistical significance. Establishment of normal whole body FDG uptake is important to establish metabolic activity of glucose in fish compared to humans for accurate interpretation of PET images<sup>25</sup>. Results indicated that fish uptake radioactive glucose in a manner similar to humans, therefore, fish could serve as replacement animals for research in diagnosis, staging, and monitoring treatment of certain types of cancers. There would also be a reduction in the number of animals that would be needed in research projects because with these advanced imaging capabilities, the same fish could be reimaged multiple times. Since fish models for various neoplasms already exist, this study provides a novel experimental method to utilize these replacement animals. This study also has important applications to the rapidly growing industry of aquaculture. By visualizing glucose uptake in the fish, we will begin the process of understanding how carbohydrates are metabolized to achieve maximum growth.

Since advanced imaging techniques do not require the sacrifice of animals, my research is harmonious with the laboratory animal edict regarding *reduction*. Application of advanced imaging techniques to fish does not require the sacrifice of animal life, as is normally the case when animal subjects are euthanized using other conventional techniques for dissection, tissue collection, and histopathology. I performed two very different studies to demonstrate the application of advanced imaging techniques to reducing animal numbers in two areas of study in which fish could be more widely used: behavioral and carcinogenesis research<sup>8,26,27</sup>.

## CHAPTER II

### THE EFFECT OF OTOLITH MALFORMATION ON BEHAVIOR AND CORTISOL LEVELS IN JUVENILE RED DRUM FISH (*Sciaenops ocellatus*)\*

#### *INTRODUCTION*

Red drum (*Sciaenops ocellatus*), a perciform teleost species of the family Sciaenidae, are commonly used for endocrine and nutrition research and are a recreationally important species common in the Gulf of Mexico and southeastern United States<sup>28</sup>. Since 1983, hatchery-reared red drum have been stocked to help restore depleted populations in Texas. Unlike other commonly cultured species like salmonids, juvenile red drum inhabit warm waters (as high as 30 °C), grow at extremely rapid rates, and are freely euryhaline. In addition, red drum have excellent aquacultural potential because they can be cultured at a range of temperatures and salinities<sup>29</sup>.

On their arrival to our institution, a new group of red drum was noted to have a specific set of phenotypic abnormalities consistent with vitamin C deficiency during the larval stage. The exact cause of the abnormalities in these fish was unknown. However, because vitamin C (ascorbic acid) is a water-soluble and heat-labile vitamin that can degrade quickly in the diet, vitamin C deficiency was a reasonable explanation for the observed deformities<sup>30</sup>. Vitamin C acts as a reducing agent and antioxidant in teleosts and is a dietary requirement for most fish, including red drum, because they are unable

---

\* Reprinted with permission from “The effect of otolith malformation on behavior and cortisol levels in juvenile red drum fish, *Sciaenops ocellatus*” by Z.S. Browning, A.A. Wilkes, E.J. Moore, T.W. Lancon, F.J. Clubb. 2012. *Comparative Medicine* 62(4), 251-256, 2012.



to synthesize it<sup>28</sup>. In addition, ascorbic acid is a cofactor in hydroxylating amino acids for collagen synthesis, which is required for wound repair, formation of connective tissue and bone matrix<sup>31</sup>. Common signs of vitamin C deficiency in teleost fish include deformities of the spine, jaw, and cephalic region as well as anophthalmia and shortened opercula<sup>32</sup>. These signs were present in all of our phenotypically abnormal fish. Because of the visible skeletal malformations of the cranium and spine, we hypothesized that the abnormal fish had abnormal otoliths, because bone deposition lesions can be associated with poor collagen formation<sup>28</sup>.

Fish hear in a similar fashion to other vertebrates<sup>33</sup>. Otoliths (or ‘ear stones’) are dense calcareous structures in the chambers associated with the ear in teleost fishes<sup>34</sup>. The saccular otolith, also called sagittal otolith or sagitta, is the largest in most fishes and is considered the primary auditory organ<sup>35</sup>. Otoliths are considered to be involved in both auditory and vestibular functions. These calcareous structures detect motion and indirectly sense fluctuations of swim-bladder volume in a pressure field. In addition, otoliths relay information about sound source characteristics, including distance and location<sup>36</sup>. The precise pattern of otolith motion likely is affected by characteristics of the otolith, including its mass and center of gravity<sup>37</sup>.

Red drum have very large otoliths and, as a result, tend to be very responsive to external stimuli<sup>35</sup>. Based on the skeletal deformities we observed, we hypothesized that these phenotypically abnormal fish would have abnormal otoliths, which would lead to behavioral differences resulting from impaired sensory function. We also hypothesized that abnormal fish would have increased acute cortisol responses compared with those of

normal fish due to a greater startle response when netted, because they are unable to hear the approach of the net<sup>29,38</sup>. The elevation of plasma corticosteroids, mainly cortisol, in teleosts in response to various types of stressful stimuli has been well documented and constitutes an important hormonal or primary response to stress<sup>39</sup>.

#### *MATERIALS AND METHODS*

Red drum were obtained as fry and grown to juvenile size (weight, 20 to 80 g) at the Aquacultural Research and Teaching Facility (Texas A and M University, College Station, TX). The standard length and wet mass (mean  $\pm$  SEM) for all fish (abnormal and normal) were  $16.5 \pm 0.8$  cm and  $76.5 \pm 1.1$  g, respectively. The abnormal and normal groups were maintained in 2 recirculating 1900-L tanks at  $25 \pm 2$  °C and 6 ppt salinity on a 12:12-h light: dark cycle and commercial fish diet. All fish were maintained and treated humanely, and experimental protocols were approved by the Texas A and M University IACUC (Institutional Animal Care and Use Committee).

Fish were separated into 2 groups with  $75 \pm 5$  fish per group; the normal group contained only physically normal red drum, whereas the other group consisted of drum with various phenotypic skeletal abnormalities. For 15 d, fish were observed once daily at 0900 for 10 min by a single impartial observer who was unaware of the purpose for monitoring and recording behavior. Fish were scaled as a group on 3 responses: schooling, response to visual stimuli (a standard commercial aquaculture feed; Rangen), and response to acoustic stimuli. Acoustic stimuli consisted of a verbal phrase spoken by the observer after she had been in the room for 5 min—long enough for the fish to acclimate to her presence<sup>29</sup>. The speaker was instructed to use the same volume, tone of

voice, and phrase during the stimulus. Groups were scored on a scale of 1 to 5 based on their responses (Table 1).

For blood collection for cortisol analysis by radioimmunoassay, 8 normal and 7 abnormal red drum were anesthetized by using tricaine methanesulfonate (MS222; Fiquel, Argent Chemical Laboratories, Redmond, WA). Blood was collected from the caudal vein and centrifuged to separate the plasma. Plasma was stored at  $-80^{\circ}\text{C}$  until cortisol analysis by using Coat-A-Count Total Cortisol kits (Siemens, Los Angeles, CA); this kit quantifies hormone concentration in diluted samples by using an antibody-coated tube method.

Another 7 abnormal and 3 normal red drum were chosen randomly and euthanized by using tricaine methanesulfonate. They were imaged with microCT (Hawk-160XI, X-Tek Group, Santa Clara, CA). MicroCT scans were reconstructed (version 2.0, VGStudio MAX, Volume Graphics, Heidelberg, Germany) for visualization and qualitative evaluation of otolith morphology. In addition, 8-bit image stacks of the microCT scans were exported to conduct quantitative microCT measurements of the total volume of both sagittal otoliths.

After imaging, all otoliths were removed, air dried, and weighed individually on a gram scale. Otolith volume was measured by water displacement in a 5-mL graduated cylinder. The information was used to calculate density by dividing weight (in grams) by volume (in milliliters). The mean behavioral scores, cortisol levels, and otolith volume, mass, and density of normal and abnormal fish were analyzed by using the Student t test

(Excel 2010, Microsoft, Redmond, WA). Differences were considered to be significant when the P value was less than 0.05.

## *RESULTS*

All of the classic signs of vitamin C deficiency, including deformities of the spine, jaw, and cephalic region, anophthalmia, and shortened opercula, were present in fish in the abnormal group. Other than their phenotypic abnormalities, the abnormal fish exhibited similar trends in weight gain and growth as those of normal fish. Over the 15-d observational period, mortality in the normal drum was 32% compared with only 2% in the abnormal fish.

The normal and abnormal fish had statistically significant ( $P < 0.05$ ) differences in behavior (Figure 1). Normal fish had more schooling behavior ( $P < 0.001$ ) and swam close together without touching, whereas abnormal fish were dispersed randomly throughout the tank. The abnormal group was more responsive ( $P < 0.04$ ) to visual stimuli of food than was the normal group. The abnormal fish swam closer to food and more quickly, whereas normal drum were slower to react to the presence of food. The abnormal group showed no response to acoustic stimuli, whereas normal fish swam away from the source of the noise ( $P < 0.001$ ). Plasma cortisol levels of the abnormal drum group were significantly ( $P < 0.001$ ) higher than those of the normal group (Figure 2).

MicroCT of abnormal red drum revealed operculum abnormalities, malocclusions due to brachygnathia or prognathia, different types of otolith malformations, and spinal deformities such as kyphosis when compared with images

from the normal group. The mean volume of abnormal sagittal otoliths was 3 times that of normal otoliths: 36.7 mm<sup>3</sup> as compared with 12.29 mm<sup>3</sup> ( $P < 0.001$ ). The sagittal otolith was the largest of the otoliths. Normal sagitta are oval, smooth on the lateral surface, rounded at the antirostral end with a well-developed sulcul ridge on the medial surface (Figure 3)<sup>28</sup>. In normal red drum, normal occlusion of the mouth was present, and the operculum was fused and fully covered the gills (Figure 3). All abnormal drum had shortened, unfused opercula and oral cavity abnormalities; many also exhibited cranial abnormalities (Figure 4). Sagittal otolith abnormalities ranged from abnormal shape, asymmetry, and abnormal ossification, with abnormal ossification being the most common (Figure 5)<sup>40</sup>.

The density of the otoliths from the normal fish was significantly ( $P < 0.001$ ) higher than of the phenotypically abnormal group; however, the volume of the otoliths was significantly ( $P < 0.001$ ) higher in the abnormal group (Figure 6). There was no significant difference in the mass of otoliths between the 2 groups ( $P = 0.922$ ), indicating that the fish were approximately the same age. A direct relationship between otolith mass and linear aging has been well documented, making otolith mass measurements a good indicator of fish age<sup>34,41,42</sup>

## *DISCUSSION*

Comparative studies on fish ear structure may facilitate research regarding how animals and humans interpret complex auditory stimuli<sup>43</sup>. By extrapolation from zebrafish studies, the simplest method to detect deficiencies in the auditory structure is to screen for defects in otolith morphology<sup>8</sup>. Because the saccular otoliths are the major

sound detector in most fish, we elected to image these structures<sup>37</sup>. We used microCT to scan 7 of the phenotypically abnormal red drum and confirmed that all 7 fish had abnormal sagittal otoliths, with the most consistent abnormality being abnormal ossification. Abnormal ossification was further confirmed by significant differences in density and volume between the 2 groups of fish. Acoustic functionality (sensitivity, temporal processing, and sound localization) is altered by otolith mass asymmetry<sup>36</sup>. We therefore hypothesized that abnormal shape and ossification of otoliths would compromise functionality and resultant behavior. We speculated that abnormal drum would demonstrate atypical behavior because these fish would be less aware of their surroundings than would be normal fish. Behavioral studies of laboratory red drum have taught us to expect consistent schooling behavior and rapid responses to acoustic stimuli<sup>29</sup>. Consistent with our hypothesis, abnormal red drum exhibited less schooling behavior and no response to acoustic stimuli, whereas normal fish showed more schooling and swam away from the acoustic source.

The abnormal fish had a greater response to visual stimuli (food) than did normal fish. This finding is consistent with the sensory compensatory mechanism described in humans<sup>44,45</sup> and cave fish, in which increased acuteness of hearing compensates for loss of vision<sup>46</sup>. The hearing capabilities of fish can be measured behaviorally<sup>37,47</sup>. Therefore, the behavior data from the current study support the hypothesis that abnormal red drum perceive their environment differently than normal red drum because the hearing capabilities of the abnormal fish have been compromised.

We further hypothesized that defects in the auditory structures and responses to stimuli would result in increased responses to stress in these fish. Cortisol is the predominant corticosteroid released in red drum during acute stress<sup>48</sup>. The elevation of plasma corticosteroids, mainly cortisol, in teleosts in response to various types of stressful stimuli has been well documented and constitutes an important hormonal or primary response to stress<sup>38,47</sup>. In addition, an appropriate corticosteroid response appears to be essential for resistance to severe trauma via the stimulation of gluconeogenesis and involvement with osmoregulation<sup>39</sup>. Handling and anesthesia are expected to result in an acute cortisol stress response that may represent a ‘fright’ reaction to a novel stimulus<sup>38</sup>. Both fish groups exhibited increased cortisol responses in response to capture as compared with published normal resting levels for red drum;<sup>48</sup> however, the cortisol levels of the abnormal fish were significantly higher than those of the normal group. We propose that the auditory impairment caused by abnormal otoliths resulted in a heightened startle response when abnormal fish were netted. This fright response may be similar to the increased startle response seen in visually impaired humans<sup>49</sup>. In addition, children with hearing loss from an adverse event have increased cortisol levels compared to children with normal hearing ability<sup>50</sup>. Fish are now well accepted to perceive sound in the same manner as do other vertebrates<sup>33</sup>.

In summary, the gross morphologic defects in the affected group of fish were only one aspect of the abnormalities present in these animals; they also had significant differences in their behavioral and cortisol responses (Table 2). Data obtained from studies with these phenotypically abnormal animals may be compromised by their

physiologic differences from normal fish. Further studies are needed to define the link between otolith deformities and vitamin C deficiency; however, vitamin C deficiency in red drum might provide a new animal model of hearing impairment.



CHAPTER III  
USING PET/CT IMAGING TO CHARACTERIZE 18 F-FLUORODEOXYGLUCOSE  
UTILIZATION IN FISH\*

*INTRODUCTION*

Fish have become increasingly valuable as research models for a number of reasons, including low cost, portability, ease of laboratory culture, and short reproductive lifecycle. As early as 1910, President Taft proposed the creation of a federal research laboratory focused on studying cancer in fish<sup>6</sup>. Since that time, many fish species have been established as animal models for human neoplasms including rainbow trout, *Oncorhynchus mykiss* (Walbaum) with hepatocellular carcinomas<sup>9</sup>, platyfish/swordtails, *Xiphophorus hellerii x variatus* (hybrid) with melanomas<sup>14</sup>, catfish, *Ameiurus nebulosus* (Lesueur) with epitheliomas<sup>15</sup> and bicolored damselfish *Stegastes partitus* (Poey) with schwannomas<sup>16</sup>. Zebrafish, *Danio rerio* (Hamilton) and medaka, *Oryzias latipes* (Temminck & Schlegel) are already being widely used in cancer research for everything from genetic screening to anticancer drug screening to transplantable tumors<sup>3-7,27,51</sup>. The novel fish neoplasia research of Mearl Stanton piqued the interest in the use of fish species for cancer research in 1965<sup>9</sup>.

Since Stanton's work, newer methods of studying carcinogenesis *in vivo* have been developed. Combined positron emission tomography/computed tomography

---

\* Reprinted with permission from "Using PET/CT Imaging to Characterize 18 F-Fluorodeoxyglucose Utilization in Fish" by Z.S. Browning, A.A. Wilkes, D.S. MacKenzie, R.M. Patterson, M.W. Lenox. 2012 *Journal of Fish Diseases*, doi:10.1111/jfd.12081.

(PET/CT) is a relatively new imaging modality that combines the functional images of PET with the anatomical information of CT. PET is capable of detecting areas of metabolic activity by using radio-labeled molecular probes with specific uptake rates. The most commonly used PET tracer is  $^{18}\text{F}$ -fluorodeoxyglucose (FDG), a glucose analogue that allows measurement and mapping of tissue glucose uptake <sup>17</sup>. FDG, like glucose, enters the cells and is phosphorylated by hexokinase to FDG-6-phosphate. Unlike glucose, FDG is not further metabolized and thus becomes trapped in the cell <sup>52,53</sup>. In normal tissues, FDG uptake peaks in the heart, liver, and kidneys shortly after administration <sup>20</sup>. In the presence of neoplasia, the tumor also takes up glucose/FDG rapidly, allowing for the visualization of the tumor mass *in vivo* over time <sup>17,20</sup>. The retention of the tracer is calculated as SUV (standard uptake value), the most widely used unit of measure of metabolic rate of glucose uptake <sup>20,52</sup>. SUVs provide highly reproducible parameters of cellular glucose metabolism, allowing for accurate comparison among PET studies <sup>17</sup>. However, the accuracy of PET measurements alone can be hampered by lack of sufficient anatomical detail. PET/CT merges the two systems, combining the images acquired from both devices into one superimposed image. Thus, functional imaging obtained by PET can be more precisely correlated with anatomic three-dimensional imaging obtained by CT scanning.

PET/CT is commonly used in cancer studies, but to date these studies rely on mammals such as dogs and rodents <sup>21,22,54</sup>. Four key areas of oncology in particular use FDG-PET imaging: grading tumors, determining tumor extent, determining prognosis, and measuring tumor response to treatment <sup>52</sup>. Tumor cells have increased metabolic

activity, and thus exhibit increased glucose uptake <sup>17,21</sup>. Therefore the glucose analogue FDG is used to map and quantify glucose use in tumors <sup>21</sup>. In the future, FDG-PET/CT imaging will likely become increasingly important by providing more accurate quantitative information than previous conventional *in vivo* methods of oncology studies <sup>52</sup>. Since laboratory animal medicine seeks to replace more sophisticated animal models with animals of lower phylogenic classification, this project has the potential to establish teleost fish as promising replacement animals for mammals in carcinogenesis research. Because FDG-PET/CT has not previously been studied in fish, the goal of this study was to show that fish can be a viable replacement animal in cancer studies by demonstrating the similarities between fish and humans in glucose uptake in select organs prior to carcinogenesis studies. In most cases, fish neoplasms are relevant to human cancers because fish neoplasia has been proven to be histologically similar to human neoplasia <sup>3,4,6</sup>, and the genetics also appears to be highly conserved <sup>3</sup>. Therefore if fish FDG uptake resembles human FDG uptake, there should little difference in the tumor metabolism. We also have the technology to graft human tumor cells onto fish meaning the tumors would be identical to human neoplasms <sup>4,7</sup>. The establishment of normal whole body FDG uptake is important to establish baseline physiological activity in fish compared to humans for accurate interpretation of PET images <sup>7</sup>. Because of known physiological variability among fish species in venous uptake and metabolism, a variety of species was chosen in the present study to encompass the three different teleost trophic classes <sup>12</sup>. The species chosen represent fish species widely used in aquaculture research. Because of the size limitation of the imaging system, only large fish could be used, not medaka or

zebrafish. With the advance of technology, it may be possible to use this technique with small fish in the near future.

#### *MATERIALS AND METHODS*

Five fish each of 7 species were used: koi, *Cyprinus carpio carpio* L., tilapia, *Oreochromis aureus* (Steindachner), hybrid striped bass, *Morone saxatilis* x *M. chrysops* (hybrid), channel catfish, *Ictalurus punctatus* (Rafinesque), red drum, *Sciaenops ocellatus* L., grass carp, *Ctenopharyngodon idella* (Valenciennes), and largemouth bass, *Micropterus salmoides* (Lacepède). The fish weighed an average of  $607.6 \pm 43.88$  grams and measured  $36.7 \pm 0.78$  cm from nose to tail (Table 3). All fish were obtained from the Aquacultural Research and Teaching Facility (ARTF) of the Texas A&M University System. This facility includes laboratories, hatcheries for red drum and other species and a 36-pond complex. Laboratories are equipped with extensive flow-through and recirculating tank systems, comprising more than 200 units, and with a variety of modern research equipment for work in areas of nutrition, bioenergetics, environmental physiology and developmental biology. Fish were maintained in recirculating 1900 L tanks at  $25 \pm 2^\circ\text{C}$ , 12L: 12D photoperiod with aeration. All fish were fed once daily with a commercial fish diet (Rangen Inc, Aquaculture Feeds, Buhl, Idaho). Water quality parameters was checked daily and maintained at pH 6.5-8.5, alkalinity >50 ppm, nitrites= 0 and ammonia=0. Red drum were kept under the same conditions as other fish except they were housed in 6 ppt salinity. On the day of the experiment fish were placed in individual, oxygenated 10 gallon plastic bags and transported from their holding tank to the imaging facility. Upon arrival, fish were sedated with 100 mg/ml FINQUEL®

(MS-222®; Pure Tricaine Methanesulfonate; Argent Chemical Laboratories, Inc., Redmond, WA) buffered with equal parts sodium bicarbonate to a neutral pH for physical examination, placement of identification tags, and collection of weights and lengths. During this time, anesthesia was maintained at stage 4, which is defined by total loss of muscle tone and equilibrium, slow and regular opercular movement and loss of spinal reflex<sup>55</sup>. Fish with significant phenotypic abnormalities noted on physical exam were excluded from the study.

The experimental protocol was approved by the Texas A&M University Institutional Animal Care and Use Committee. Fish were fasted for 24 hours prior to the experiment, in accordance with general PET imaging guidelines. FDG was injected intravenously as a bolus in the caudal vein. FDG activity in the syringe was quantified before and after FDG injection, and recorded together with time measurements. The measurement was obtained in millicuries (mCi) and converted to Becquerel (Bq), and the decay-corrected activity was calculated. All fish were imaged with combined PET/CT at 30 and 60 minutes post injection. All imaging was accomplished under MS-222® stage 4 anesthesia with minimal time spent out of water. Fish were out of the water for approximately 6 minutes per scan, with actual scanning time taking 5 minutes. The fish recovered without complications after the first scan and were euthanized by overdose of MS-222® followed by cervical dislocation immediately following the second scan at 60 minutes.

Whole body PET/CT was performed using a 128 slice Siemens Biograph mCT scanner (SOMATOM Definition AS+, Siemens Medical Solutions USA, Inc.) as

described by Jakoby et al <sup>18</sup>. The CT parameters were a slice thickness of 0.6 mm, 120 kv, 340 mas, pitch 0.6, H31s medium smooth filter kernel. PET scans were acquired using 3D acquisition mode, and PET data were attenuation corrected based on CT data <sup>19</sup>.

All acquired PET images were reconstructed using a 3D OSEM reconstruction with point spread function modeling and time of flight compensation (3 iterations, 21 subsets). The reconstructed images were smoothed using a Gaussian filter setting for FWHM of 3.0 mm in all directions, and a matrix size of 400 x 400 and a physical pixel size of 0.3571 mm. Measured FDG activity in all field of view positions was attenuation corrected to the start time of the whole body PET scan.

The PET/CT images were transferred for post-processing to the Siemens workstation. All PET/CT images were evaluated subjectively and regions of interest (ROI) for semi-quantitative analysis were drawn manually. The program automatically calculated and reported the mean, minimum, and maximum of FDG activity per volume within ROIs on the co-registered PET/CT images.

ROIs were drawn to evaluate liver, brain, heart, gastrointestinal tract, trunk kidney, and dorsal lumbar musculature. Organ ROIs were drawn manually on the transverse or sagittal images, and 3-dimensional position was confirmed on the axial images. All ROIs were drawn to include the largest area of the region or organ in the individual image.

FDG SUV for each organ was calculated by dividing the averaged attenuation-corrected ROI activity (Bq) per tissue in cm<sup>3</sup> by the injected activity (Bq)/body weight

(g). Radioactive decay was corrected to the start time of the PET scans using the

following equation:  $dose_{corrected} = dose_{initial} * 2^{\left(\frac{T_{scan} - T_{assay}}{T_{HL}}\right)}$

$T_{scan}$  is the time the fish was imaged.  $T_{assay}$  is the time the radiation level of the FDG was tested. The half-life of FDG ( $T_{HL}$ ) is 109.7 minutes.

The mean SUV and standard error measurement for the ROI (heart, liver, brain, dorsal lumbar musculature, and kidney) in each species of fish at two time points (30 minute and 60 minute) were calculated. The mean values for each teleost species were compared both separately and as a group of all fish species to published human values<sup>25</sup> using the z-test for two sample means. A p-value of less than 0.05 was used to define significance. Published values of SUV for the same ROI in dogs<sup>21</sup> and mice<sup>54</sup> were compared to humans using the z-test for two sample means (Excel).

## *RESULTS*

A mean activity of  $1.10^7$  Bq (range  $6.66^6$ - $1.52^7$  Bq) FDG was injected into each fish. FDG uptake into specific organs at 30 minutes was easily detectable and quantifiable (Figure 7). Multiple fish could be simultaneously imaged in a single 5 minute scan by placing them together on the scanning bed (Figure 8). Although the images shown are two dimensional snapshots of these animals, a powerful benefit of the technology was its three dimensional capabilities allowing for elimination of superimposition artifacts. ROI SUV mean and standard error measurement from fish species are listed according to the time point at which they were imaged, 30 verses 60 minutes post injection (Tables 4 and 5). Data for the imaging analysis of largemouth bass at 60 minutes is unavailable due to a processing error during imaging.

The SUVs of individual fish species and fish as a group were more similar to humans at thirty minutes than at sixty; therefore, all further discussion refers to the thirty minute data (z-test,  $p > 0.05$ ). Because there were no significant differences in the ROIs between individual fish species, we combined all fish into a single group for analysis. As in mammalian studies, our results were decay corrected for time elapsed post injection. No significant differences in SUV were found between fish and humans in any of the ROIs (Figure 9,  $p > 0.05$ ). Interestingly, while values for fish taken as a group were not significantly different from humans, within fish species, fish classified as carnivores (red drum and bass species) had higher standard errors as compared to the herbivores and omnivores (Tables 4 and 5). In all fish, measureable uptake was observed in the brain, heart, liver, and trunk kidney. The gastrointestinal tract of all fish was characterized by moderate to high uptake. However, the SUVs for the GI tract were not used for comparison to humans due to the complicating effects of peristalsis and the variability of the GI tract among fish species; in most species, peristalsis makes SUV measurement of the gastrointestinal tract unreliable<sup>22</sup>. All fish showed unexpectedly elevated SUVs in the tail muscle. This uptake was likely caused by arterial delivery of FDG from the injection site or movement of the animal during the uptake period. Moderate uptake was also observed on the anterior jaw of many fish, possibly due to inflammation from trauma during anesthesia and transport<sup>23,53</sup>. Fish were free from external abnormalities prior to handling. However, post transport and anesthesia, red lesions were observed on the anterior jaw of some fish due to their thrashing movements. The lowest uptake



values in the fish were observed in the dorsal lumbar musculature, as is common in most species<sup>20,25,54</sup>.

The ROIs were chosen because they represent the major organ systems of interest in the regulation of glucose metabolism. Of all species analyzed, fish exhibited SUVs most similar to humans in the liver and brain ( $p>0.05$ ) (Figure 10). In the heart, fish and dogs were both statistically similar to humans. Similarly, uptake in the kidney of both fish and mice were statistically similar to humans. Only mice had muscle values that were significantly different from the human ( $p<0.05$ ) (Figure 10). Thus, compared to the typical animal models of dogs and mice, fish were the only species to show no significant differences in SUV from humans in all of the major organ systems (Figure 10). In addition, the 95% confidence intervals for fish and humans overlapped in all ROIs (Figure 9).

## *DISCUSSION*

Modern imaging techniques, specifically FDG-PET/CT, have revolutionized the study of oncology, particularly in the areas of screening, staging, diagnosing, measuring response, and surveying tumors<sup>17</sup>. PET quantification using SUV has been conclusively established as a useful tool for neoplasia research<sup>20</sup>. A major limitation in this imaging technique is its dependence on mammalian models. When mechanistically possible, the use of fish offers a feasible alternative model which may have more similarity to the human than mammalian models in some parameters such as cell specific rates of glucose uptake. Fish are already widely used in the field of oncology to study anticancer drugs<sup>5</sup>, monitor environmental carcinogenesis<sup>27</sup>, study cancer genetics<sup>3</sup>, transplant human

tumors <sup>4,5</sup>, as well as many other areas. However, they have not before been studied with FDG-PET/CT. The comparatively lower cost is one of the obvious advantages to using fish, but significant others include greater availability of the animals, easier maintenance, and less stringent housing density requirements. Perhaps most importantly, they offer the potential replacement of mammalian species as models <sup>9</sup>.

All fish images obtained with this technique were of high resolution, straightforward to analyze, and easily reproducible. When comparing FDG uptake in fish versus humans in major organ systems (brain, liver, heart, kidney, and muscle), the group consisting of all fish analyzed was not significantly different from humans in any of the studied organ systems. When fish were compared to humans according to their trophic level classification, there were still no significant differences. In addition, SUV values for neither omnivorous nor herbivorous fish were significantly different from human values reported in the literature. However, fish classified as carnivores (red drum and bass species) displayed greater variability in SUV measurements than omnivorous and herbivorous fish. This variability suggests that carnivorous fish may be less suitable as model species for use with FDG-PET/CT than their omnivorous and herbivorous counterparts. The greater variability may be partially explained by the proposal that carnivorous fish are “glucose intolerant” <sup>56</sup>, with the longer times required to clear a glucose load in more carnivorous fish <sup>13,24,57</sup> contributing to variability in glucose uptake. Imaging with PET/CT generally utilizes larger animals such as dogs; however, with microPET, it is also possible to use mice. When comparing human SUV values to those of dogs or mice, there is a high degree of difference in select organs including heart,

liver, brain, and kidney. These results suggest that fish could actually provide a useful alternative model for the pathogenesis of neoplasia using this technique because the FDG uptake in fish species is not significantly different from human FDG uptake across all organ systems. In addition, the 95% confidence intervals for fish and humans overlapped in all ROIs (Figure 9). A possible explanation for this similarity is the elimination of the mammalian variability in blood glucose uptake caused by insulin regulation. In mammals, FDG uptake into cells, like glucose, is primarily facilitated by insulin<sup>20</sup>. Therefore, variation in blood glucose and insulin levels could affect the uptake of FDG. In fish, this variation may be minimized because blood glucose is metabolized at a more constant rate<sup>24,57</sup> through non-insulin dependent constitutive glucose uptake. However, the genes for glucose transporters (particularly GLUT-1, GLUT-4) are well-conserved across mammalian and aquatic species<sup>11,26</sup>, suggesting that PET/CT application to fish could serve as both a viable model for carcinogenesis and offer value to aquaculture researchers interested in fish metabolism, hormonal control of glucose utilization, and feed efficiency. Additionally, screening for environmental carcinogenesis would be greatly enhanced by this technology. Assays using fish have been found to be more sensitive to carcinogens, less expensive, and faster to perform than rodent studies<sup>51</sup>. Live scanning would eliminate sacrifice of healthy animals and allow for more precise localization of tumors in afflicted animals. Although only large fish could be used due to the size limitation of this technique, with the advance of technology, it may be possible to use this technique with zebrafish and medaka in the near future.

Two complimentary factors suggest the suitability of fish as animal models in future studies. First, a key goal of laboratory animal medicine is to reduce the use of mammalian species in research. Secondly, FDG-PET/CT is quickly becoming vital in oncology research. Our study demonstrates that, with this novel technique, fish can potentially serve as highly useful adjuncts to traditional mammalian models in the study of oncology, and in some situations, can provide wholly unique approaches.

## CHAPTER IV

### SUMMARY AND CONCLUSION

My goal has been to draw on evidence provided by two different fish imaging techniques to demonstrate the scope for imaging techniques in fish. Fish have become increasingly valuable both as biomedical research models and in aquaculture research<sup>10</sup>. No other vertebrate organism offers the same combination of transparent and accessible embryos, cost-effective mutagenesis screening, sequenced genome, GFP, and knockout technology<sup>3,4</sup>. A key goal of laboratory animal medicine is to replace the use of mammalian species in research<sup>1</sup>. Fish meet this goal because, in many scenarios, fish can serve as highly useful adjuncts to traditional mammalian models, and in some situations, can provide wholly unique approaches<sup>2</sup>. However, fish have been severely underutilized in the field of advanced imaging. Although many images of fish have been captured through the use of CT (computed tomography), radiographs, and ultrasound, these images have been primarily utilized for anatomical study. Current research has neglected the potential to apply advanced imaging techniques to functional studies. I attempted to fill that gap by demonstrating first use of PET imaging in fish, and the use of CT imaging to reach functional conclusions by linking imaging data to fish behavior and physiology.

In the first experiment, microCT was used to characterize otolith deformity in vitamin C deficient captive-raised red drum. The auditory impairment observed in the abnormal fish and assessed by microCT caused behavioral and physiologic cortisol

responses analogous to the increased startle response and physiologic cortisol response seen in visually impaired humans<sup>50</sup>. There is the potential to use vitamin C deficiency to create fish with deformed otoliths, confirm and quantify the otolith changes via CT, and then study behavioral, hormonal, and physiologic responses in more detail. One day this new fish animal model could help us further understand and treat human hearing disability.

In the second experiment, FDG-PET/CT was used to quantify glucose uptake in select organs. Glucose uptake values were established for all the major organs in seven species of fish. Fish images obtained with the advance imaging techniques were of high resolution and straightforward to analyze. The data is easily reproducible and consistent across fish species. When comparing human SUV values to fish, there is no significant difference in select organs including heart, liver, brain, and kidney<sup>23</sup>. These results suggest that fish could actually provide a useful alternative model for the pathogenesis of human neoplasia. My study demonstrates that, with this novel technique, fish can potentially serve as highly useful adjuncts to traditional mammalian models in the study of oncology, and in some situations, can provide wholly unique approaches.

The applications for these imaging techniques encompass far more than the scope of this paper and include bone density measurements, organ analysis, metabolic studies, and studies with other radioactive isotopes such as radioactive iodine. PET/CT application to fish could offer value to aquaculture researchers interested in fish metabolism, hormonal control of glucose utilization, and feed efficiency. Additionally, screening for environmental carcinogenesis would be greatly enhanced by this

technology. Assays using fish have been found to be more sensitive to carcinogens, less expensive, and faster to perform than rodent studies<sup>51</sup>. Live scanning of animals eliminates waste of healthy animals and reduces numbers of animals used, another key edict of laboratory animal medicine<sup>11</sup>.

## REFERENCES

1. Russell WMS, Burch RL, Hume CW. *The principles of humane experimental technique*: Methuen and Co. Ltd, London, 1958.
2. Ostrander GK. *The laboratory fish*: Elsevier, Baltimore, Maryland, 2000.
3. Berghmans S, Jette C, Langenau D, et al. Making waves in cancer research: new models in the zebrafish. *Biotechniques* 2005;39:227-237.
4. Goessling W, North TE, Zon LI. New waves of discovery: modeling cancer in zebrafish. *Journal of Clinical Oncology* 2007;25:2473-2479.
5. Oh ES, Park SH, Chang YT, et al. A novel zebrafish human tumor xenograft model validated for anti-cancer drug screening. *Molecular BioSystems* 2012;8:1930-1939.
6. Stern HM, Zon LI. Cancer genetics and drug discovery in the zebrafish. *Nature Reviews Cancer* 2003;3:533-539.
7. Taylor AM, Zon LI. Zebrafish tumor assays: the state of transplantation. *Zebrafish* 2009;6:339-346.
8. Whitfield TT. Zebrafish as a model for hearing and deafness. *Journal of Neurobiology* 2002;53:157-171.
9. Bailey GS, Williams DE, Hendricks JD. Fish models for environmental carcinogenesis: the rainbow trout. *Environmental Health Perspectives* 1996;104:5-21.
10. Gjedrem T, Robinson N, Rye M. The importance of selective breeding in aquaculture to meet future demands for animal protein: A review. *Aquaculture* 2012; 330:117-129.
11. Díaz M, Antonescu CN, Capilla E, et al. Fish glucose transporter (GLUT)-4 differs from rat GLUT4 in its traffic characteristics but can translocate to the cell surface in response to insulin in skeletal muscle cells. *Endocrinology* 2007;148:5248-5257.
12. Nelson LE, Sheridan MA. Gastroenteropancreatic hormones and metabolism in fish. *General and Comparative Endocrinology* 2006;148:116-124.



13. Polakof S, Álvarez R, Soengas JL. Gut glucose metabolism in rainbow trout: implications in glucose homeostasis and glucosensing capacity. *American Journal of Physiology-Regulatory, Integrative and Comparative Physiology* 2010;299:R19-R32.
14. Walter RB, Kazianis S. Xiphophorus interspecies hybrids as genetic models of induced neoplasia. *Institute for Laboratory Animal Research Journal* 2001;42:299-321.
15. Lucké B, Schlumberger H. Transplantable epitheliomas of the lip and mouth of catfish I. Pathology. Transplantation to anterior chamber of eye and into cornea. *The Journal of Experimental Medicine* 1941;74:397-408.
16. Schmale MC, Hensley G, Udey L. Neurofibromatosis, von Recklinghausen's disease, multiple schwannomas, malignant schwannomas. Multiple schwannomas in the bicolor damselfish, *Pomacentrus partitus* (pisces, pomacentridae). *The American Journal of Pathology* 1983;112:238-241.
17. Boss DS, Olmos RV, Sinaasappel M, et al. Application of PET/CT in the development of novel anticancer drugs. *The Oncologist* 2008;13:25-38.
18. Jakoby B, Bercier Y, Conti M, et al. Physical and clinical performance of the mCT time-of-flight PET/CT scanner. *Physics in Medicine and Biology* 2011;56:2375-2389.
19. Kinahan P, Townsend D, Beyer T, et al. Attenuation correction for a combined 3D PET/CT scanner. *Medical Physics* 1998;25:2046-2054.
20. Landau BR, Spring-Robinson CL, Muzic RF, et al. 6-Fluoro-6-deoxy-D-glucose as a tracer of glucose transport. *American Journal of Physiology-Endocrinology and Metabolism* 2007;293:E237-E245.
21. Lee MS, Lee AR, Jung MA, et al. Characterization of physiologic 18F-FDG uptake with PET-CT in dogs. *Veterinary Radiology and Ultrasound* 2010;51:670-673.
22. Hansen AE, McEvoy F, Engelholm SA, et al. FDG PET/CT imaging in canine cancer patients. *Veterinary Radiology and Ultrasound* 2011;52:201-206.
23. Boellaard R, Oyen WJG, Hoekstra CJ, et al. The Netherlands protocol for standardisation and quantification of FDG whole body PET studies in multi-centre trials. *European Journal of Nuclear Medicine and Molecular Imaging* 2008;35:2320-2333.

24. Moon TW. Glucose intolerance in teleost fish: fact or fiction? *Comparative Biochemistry and Physiology Part B: Biochemistry and Molecular Biology* 2001;129:243-249.
25. Ramos CD, Erdi YE, Gonen M, et al. FDG-PET standardized uptake values in normal anatomical structures using iterative reconstruction segmented attenuation correction and filtered back-projection. *European Journal of Nuclear Medicine and Molecular Imaging* 2001;28:155-164.
26. Hrytsenko O, Pohajdak B, Xu BY, et al. Cloning and molecular characterization of the glucose transporter 1 in tilapia (*Oreochromis niloticus*). *General and Comparative Endocrinology* 2010;165:293-303.
27. Okihiro MS, Hinton DE. Progression of hepatic neoplasia in medaka (*Oryzias latipes*) exposed to diethylnitrosamine. *Carcinogenesis* 1999;20:933-940.
28. David A, Isely J. Differences between the sagitta, lapillus, and asteriscus in estimating age and growth in juvenile red drum, *Sciaenops ocellatus*. *Fishery Bulletin* 1994;92:509-515.
29. Smith ME, Fuiman LA. Behavioral performance of wild-caught and laboratory-reared red drum *Sciaenops ocellatus* (Linnaeus) larvae. *Journal of Experimental Marine Biology and Ecology* 2004;302:17-33.
30. Dabrowski K, Hinterleitner S, Sturmbauer C, et al. Do carp larvae require vitamin C? *Aquaculture* 1988;72:295-306.
31. Lewis-McCrea L, Lall SP. Effects of phosphorus and vitamin C deficiency, vitamin A toxicity, and lipid peroxidation on skeletal abnormalities in Atlantic halibut (*Hippoglossus hippoglossus*). *Journal of Applied Ichthyology* 2010;26:334-343.
32. Chávez de Martínez MC. Vitamin C requirement of the Mexican native cichlid *Cichlasoma urophthalmus* (Gunther). *Aquaculture* 1990;86:409-416.
33. Popper AN, Fay RR. Sound detection and processing by fish: critical review and major research questions (Part 2 of 2). *Brain, Behavior and Evolution* 1993;41:26-38.
34. Baker Jr MS, Wilson CA, VanGent DL. Testing assumptions of otolith radiometric aging with two long-lived fishes from the northern Gulf of Mexico. *Canadian Journal of Fisheries and Aquatic Sciences* 2001;58:1244-1252.

35. Paxton JR. Fish otoliths: do sizes correlate with taxonomic group, habitat and/or luminescence? *Philosophical Transactions of the Royal Society of London Series B: Biological Sciences* 2000;355:1299-1303.
36. Lychakov D, Rebane Y, Lombarte A, et al. Fish otolith asymmetry: morphometry and modeling. *Hearing Research* 2006;219:1-11.
37. Popper AN, Lu Z. Structure–function relationships in fish otolith organs. *Fisheries Research* 2000;46:15-25.
38. Thomas P, Robertson L. Plasma cortisol and glucose stress responses of red drum (*Sciaenops ocellatus*) to handling and shallow water stressors and anesthesia with MS-222, quinaldine sulfate and metomidate. *Aquaculture* 1991;96:69-86.
39. Barton BA, Iwama GK. Physiological changes in fish from stress in aquaculture with emphasis on the response and effects of corticosteroids. *Annual Review of Fish Diseases* 1991;1:3-26.
40. Secor DH, Dean JM, Laban EH. *Manual for otolith removal and preparation for microstructural examination*: Electric Power Research Institute, California, 1991.
41. Araya M, Cubillos LA, Guzmán M, et al. Evidence of a relationship between age and otolith weight in the Chilean jack mackerel, *Trachurus symmetricus murphyi* (Nichols). *Fisheries Research* 2001;51:17-26.
42. Megalofonou P. Comparison of otolith growth and morphology with somatic growth and age in young-of-the-year bluefin tuna. *Journal of Fish Biology* 2006;68:1867-1878.
43. Ramcharitar J, Higgs DM, Popper AN. Sciaenid inner ears: a study in diversity. *Brain, Behavior and Evolution* 2001;58:152-162.
44. Arno P, De Volder AG, Vanlierde A, et al. Occipital activation by pattern recognition in the early blind using auditory substitution for vision. *Neuroimage* 2001;13:632-645.
45. Noppeney U. The effects of visual deprivation on functional and structural organization of the human brain. *Neuroscience and Biobehavioral Reviews* 2007;31:1169-1180.
46. Yasuda K. Comparative studies on the swimming behaviour of the blind cave fish and the goldfish. *Comparative Biochemistry and Physiology Part A: Physiology* 1973;45:515-527.

47. Smith ME, Kane AS, Popper AN. Noise-induced stress response and hearing loss in goldfish (*Carassius auratus*). *Journal of Experimental Biology* 2004;207:427-435.
48. Robertson L, Thomas P, Arnold C, et al. Plasma cortisol and secondary stress responses of red drum to handling, transport, rearing density, and a disease outbreak. *The Progressive Fish-Culturist* 1987;49:1-12.
49. Grillon C, Pellowski M, Merikangas KR, et al. Darkness facilitates the acoustic startle reflex in humans. *Biological Psychiatry* 1997;42:453-460.
50. Singhi SC, Bansal A. Serum cortisol levels in children with acute bacterial and aseptic meningitis. *Pediatric Critical Care Medicine* 2006;7:74-78.
51. Kissling GE, Bernheim NJ, Hawkins WE, et al. The utility of the guppy (*Poecilia reticulata*) and medaka (*Oryzias latipes*) in evaluation of chemicals for carcinogenicity. *Toxicological Sciences* 2006;92:143-156.
52. Hutchinson O, Collingridge DR, Barthel H, et al. Pharmacodynamics of radiolabelled anticancer drugs for positron emission tomography. *Current Pharmaceutical Design* 2003;9:931-944.
53. Liu P, Huang G, Dong S, et al. Kinetic analysis of experimental rabbit tumour and inflammation model with 18F-FDG PET/CT. *Nuklearmedizin* 2009;48:153-158.
54. Zheng X, Yu CL, Sha W, et al. Study of an image-derived SUV and a modified SUV using mouse FDG-PET. *Nuclear Medicine and Biology* 2011;38:353-362.
55. Carter KM, Woodley CM, Brown RS. A review of tricaine methanesulfonate for anesthesia of fish. *Reviews in Fish Biology and Fisheries* 2011;21:51-59.
56. López-Olmeda J, Egea-Álvarez M, Sánchez-Vázquez F. Glucose tolerance in fish: Is the daily feeding time important? *Physiology and Behavior* 2009;96:631-636.
57. Rawles S, Smith S, Gatlin D. Hepatic glucose utilization and lipogenesis of hybrid striped bass (*Morone chrysops* × *Morone saxatilis*) in response to dietary carbohydrate level and complexity. *Aquaculture Nutrition* 2008;14:40-50.

## APPENDIX A

Figure 1. Behavioral Comparison. Behavioral differences between abnormal and normal red drum were quantified for 2 weeks by an unbiased observer using the previously described scoring system. Compared with normal fish, abnormal fish had significantly (\*,  $P < 0.05$ ) higher scores for each of the 3 criteria.

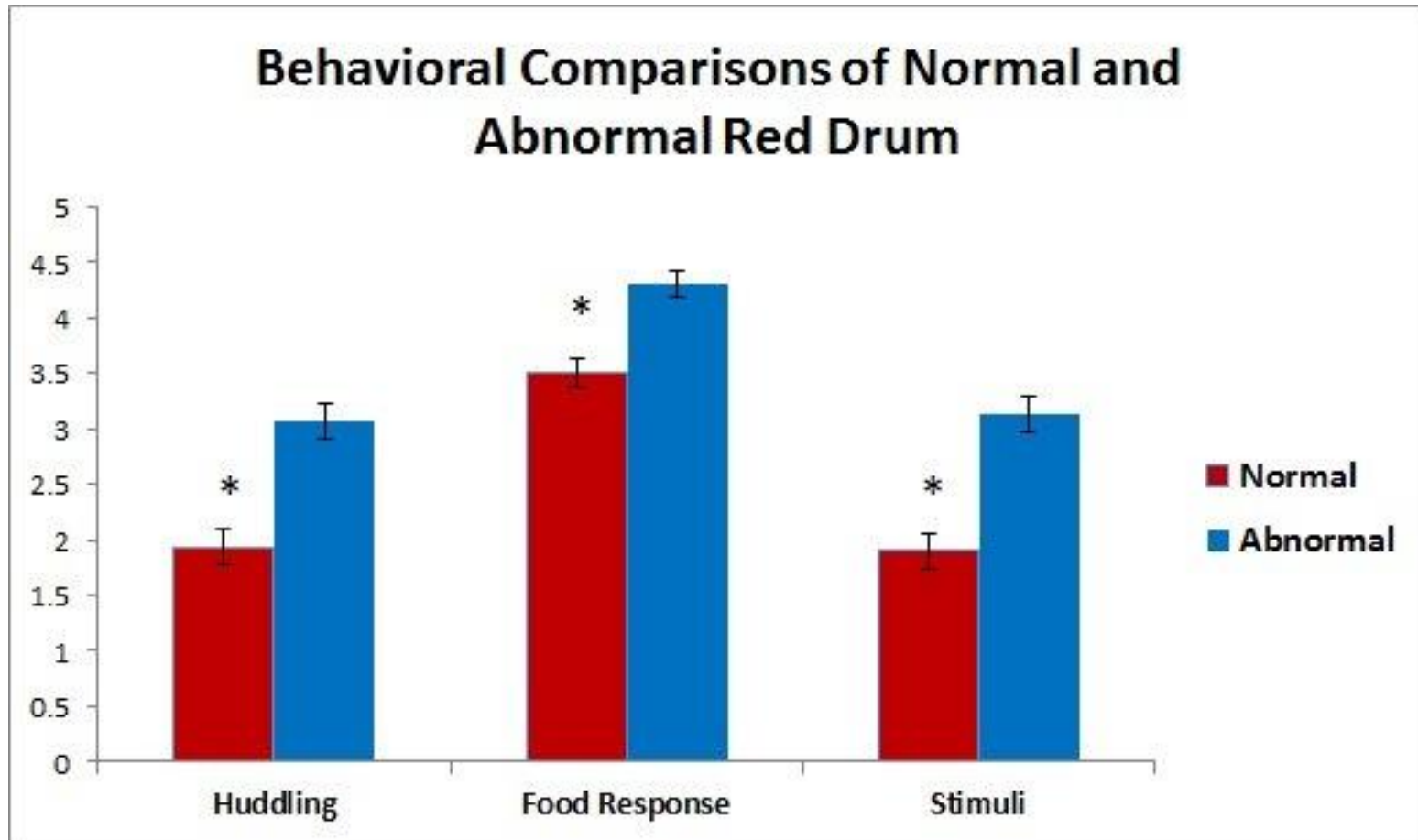


Figure 2. Cortisol Comparison. Radioimmunoassay of collected fish plasma indicated that abnormal fish had significantly (\*,  $P < 0.05$ ) higher cortisol levels than did normal fish.

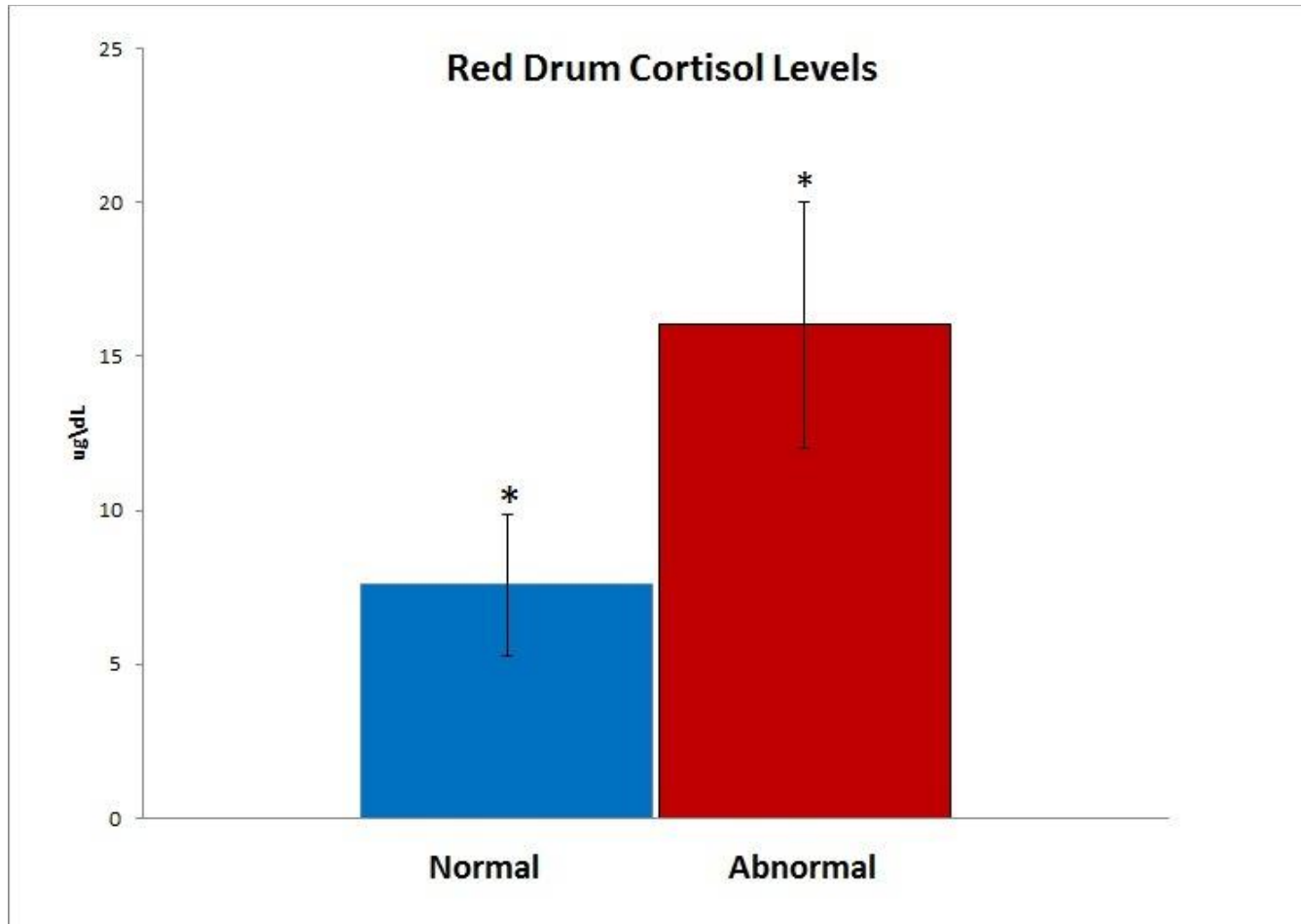


Figure 3. MicroCT of Normal Drum. MicroCT of normal red drum with normal sagittal otoliths. Head and otolith morphology were consistent among all normal fish. Arrows indicate the typical formation of normal operculum.

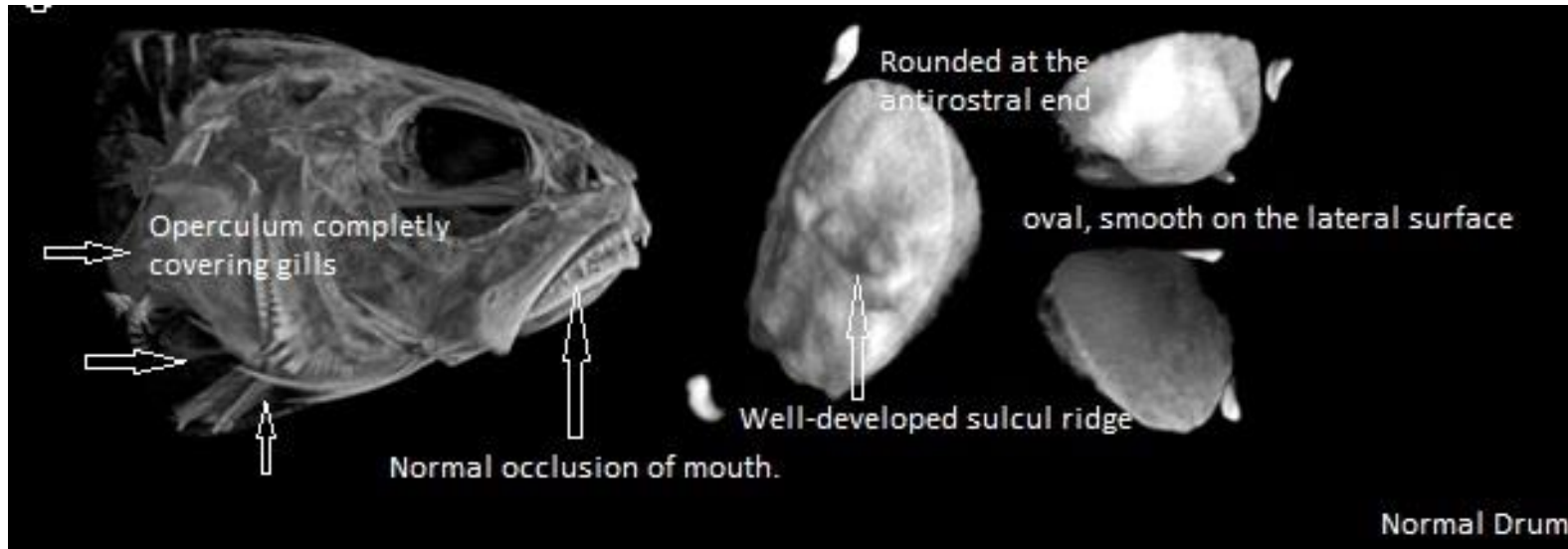




Figure 4. MicroCT of Abnormal Drum. MicroCT of abnormal red drum illustrating the most common abnormalities seen, including prognathia, brachygnathia, cranial abnormalities, and shortened and unfused operculum (delineated by arrows).

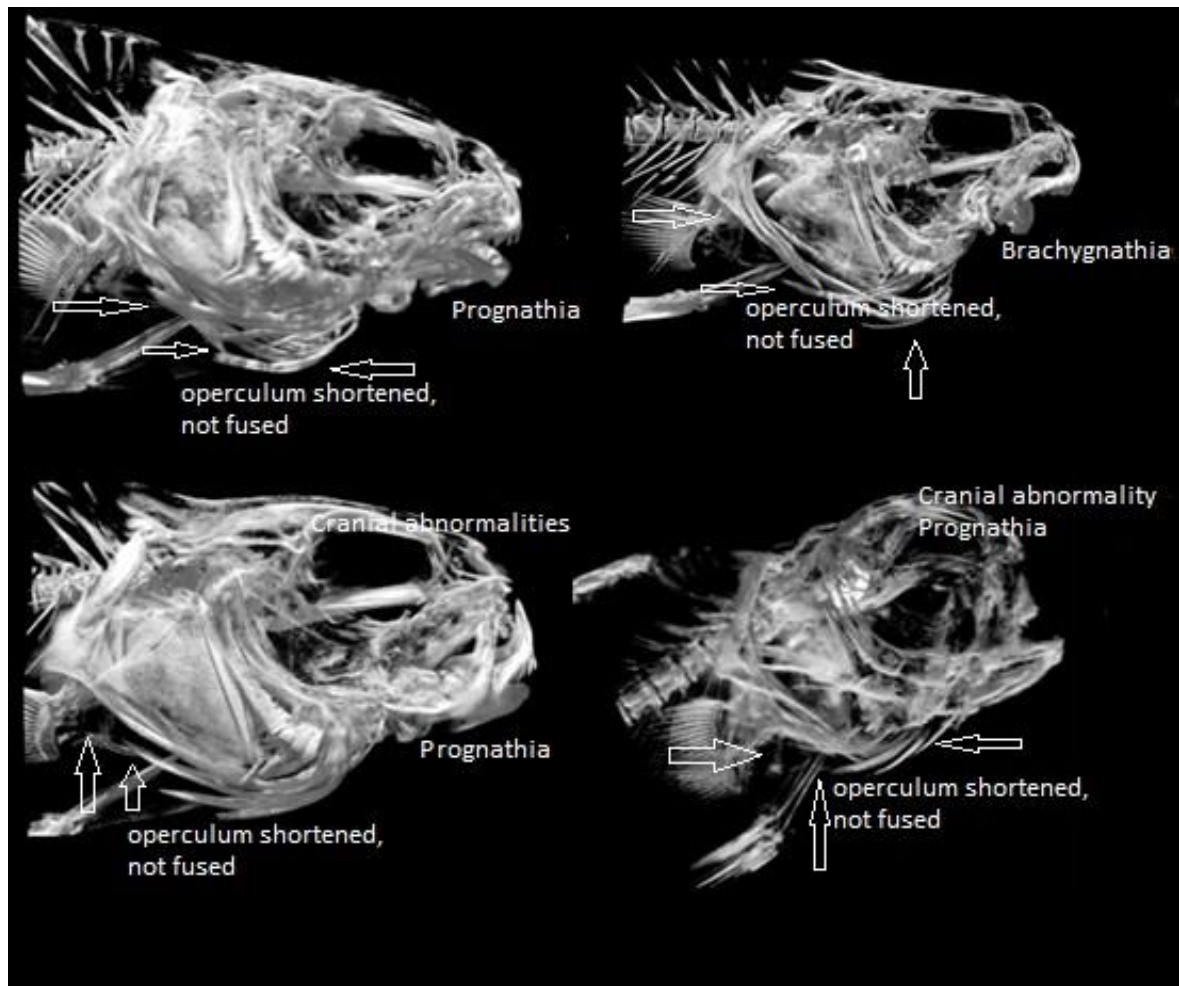


Figure 5. MicroCT of Abnormal Drum Otoliths. MicroCT of abnormal drum otoliths illustrating the most common otolith abnormalities seen, including abnormal ossification, excessive ossification of the sulcul ridge, and asymmetry of the right and left otoliths.

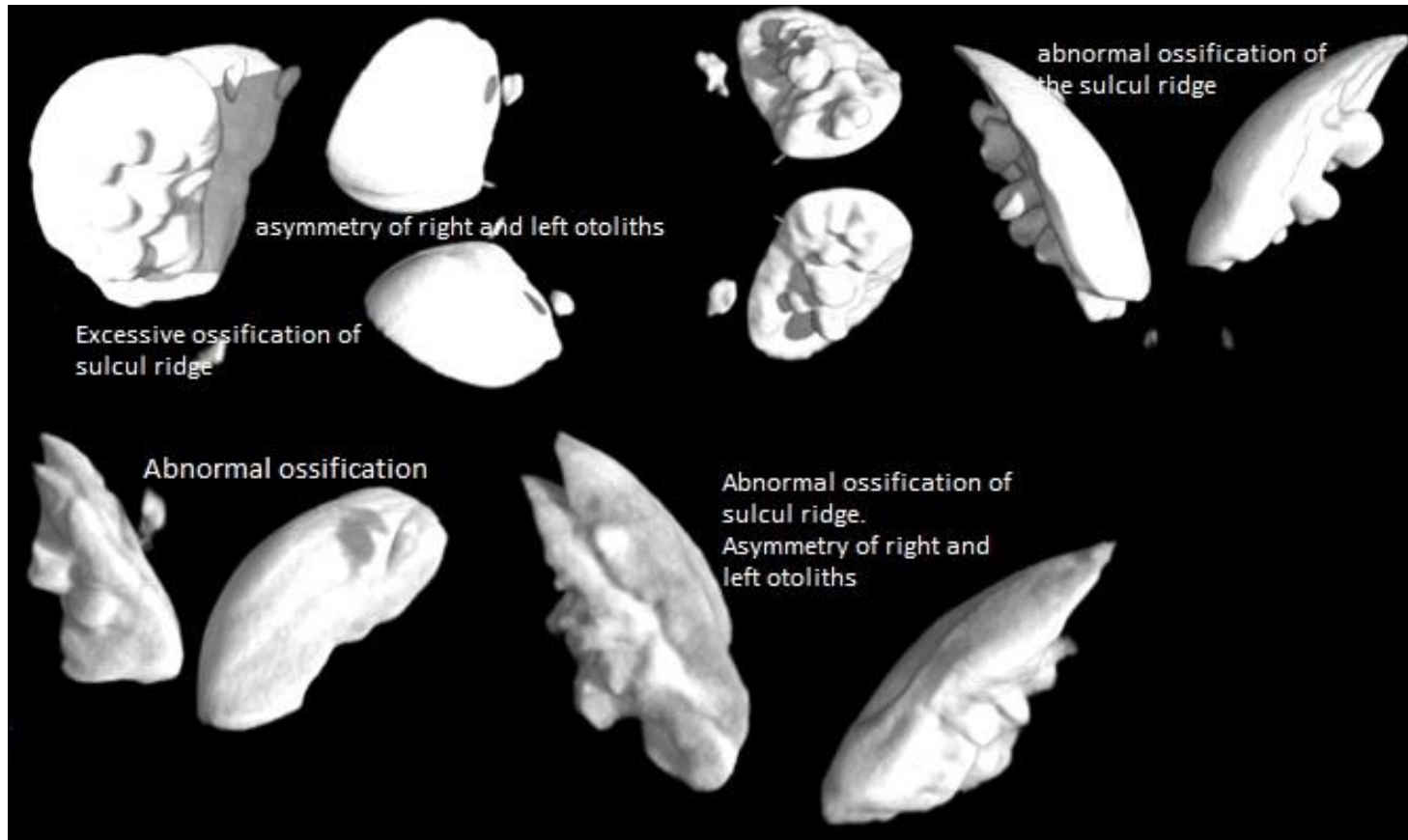


Figure 6. Otolith Comparison. Abnormal fish had significantly ( $\ddagger$ ,  $P < 0.001$ ) lower mean otolith density and higher mean otolith volume, as compared with the normal group. Mean otolith mass was similar ( $P = 0.922$ ) between the 2 groups.

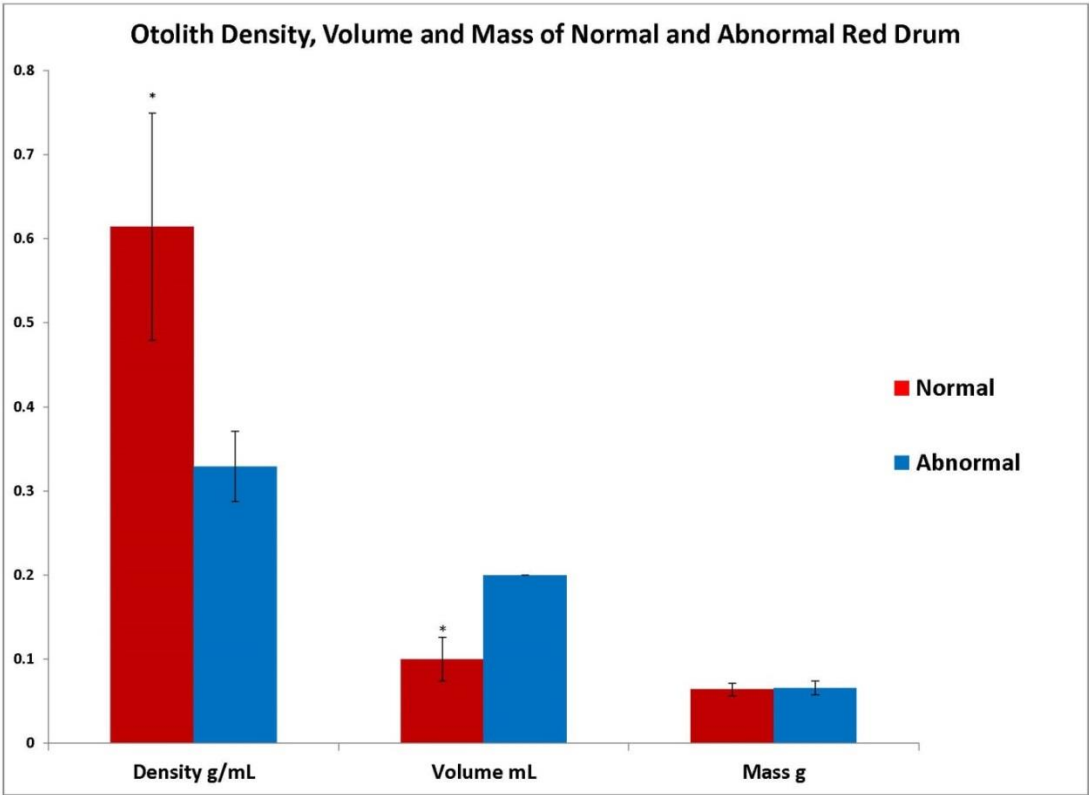


Figure 7: Tilapia FDG-PET/CT Image. FDG-PET/CT image of a tilapia thirty minutes post injection. Anatomical landmarks are indicated. The colored areas reflect glucose uptake rates, with red being the greatest followed by yellow, green, and blue. Organ ROIs were drawn manually on the transverse or sagittal images, and 3D position was confirmed on the axial images. All ROIs were drawn to include the largest area of the region or organ in the individual image. SUV analysis is performed in three dimensions, eliminating superimposition of organs apparent on this static, two dimensional image.

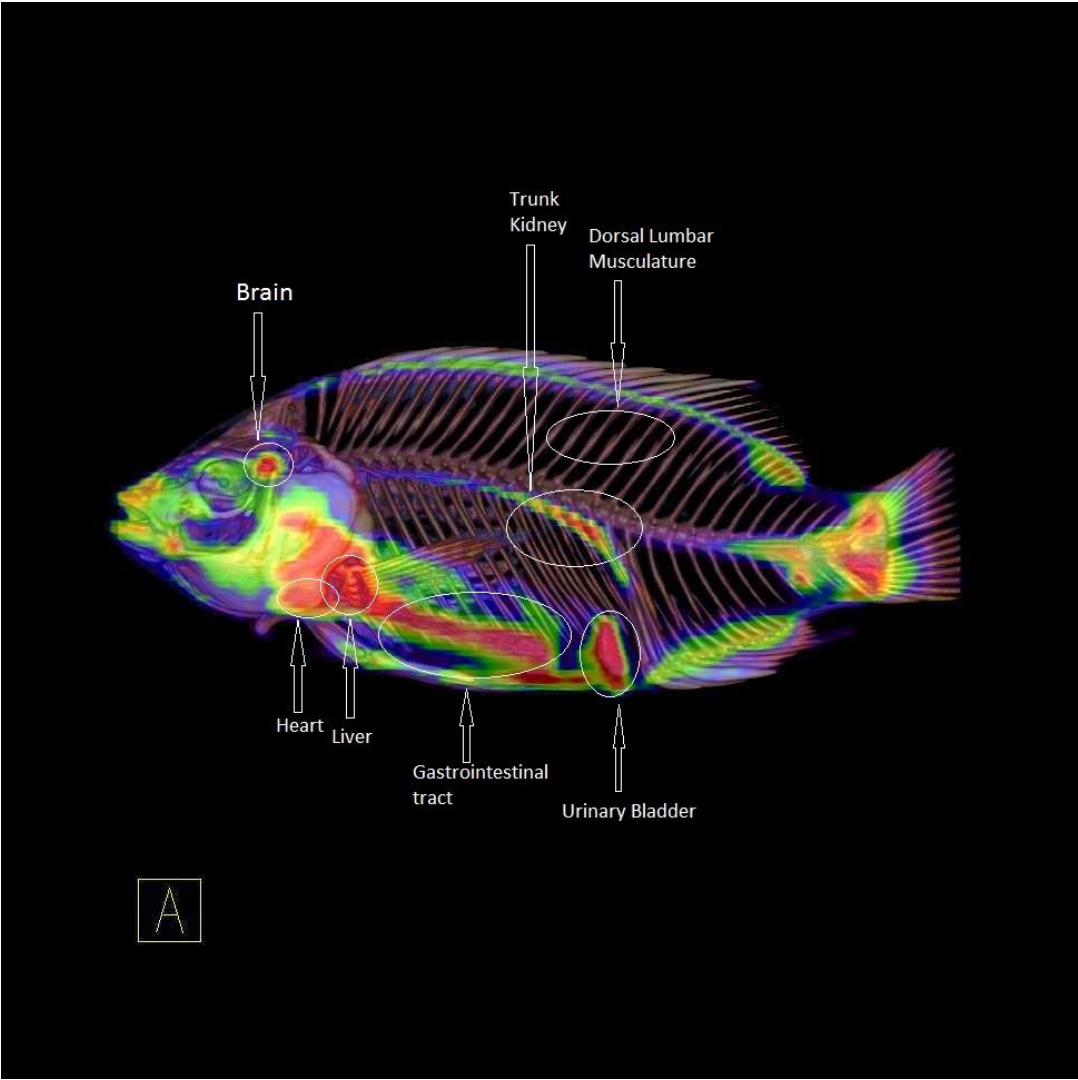


Figure 8: Red Drum Group FDG-PET/CT Image. FDG-PET/CT image of a red drum thirty minutes post injection. The drum were imaged as a group in a single scan with no increase in scan time. Apparent, intraspecific variability on this image arises partly from size variation, as fish are viewed in different planes when imaged as a group. Although there is some intraspecific variability, it is not as significant as it appears on this static, 2-d image. Three dimensional technology and individual analysis eliminates this artifact.

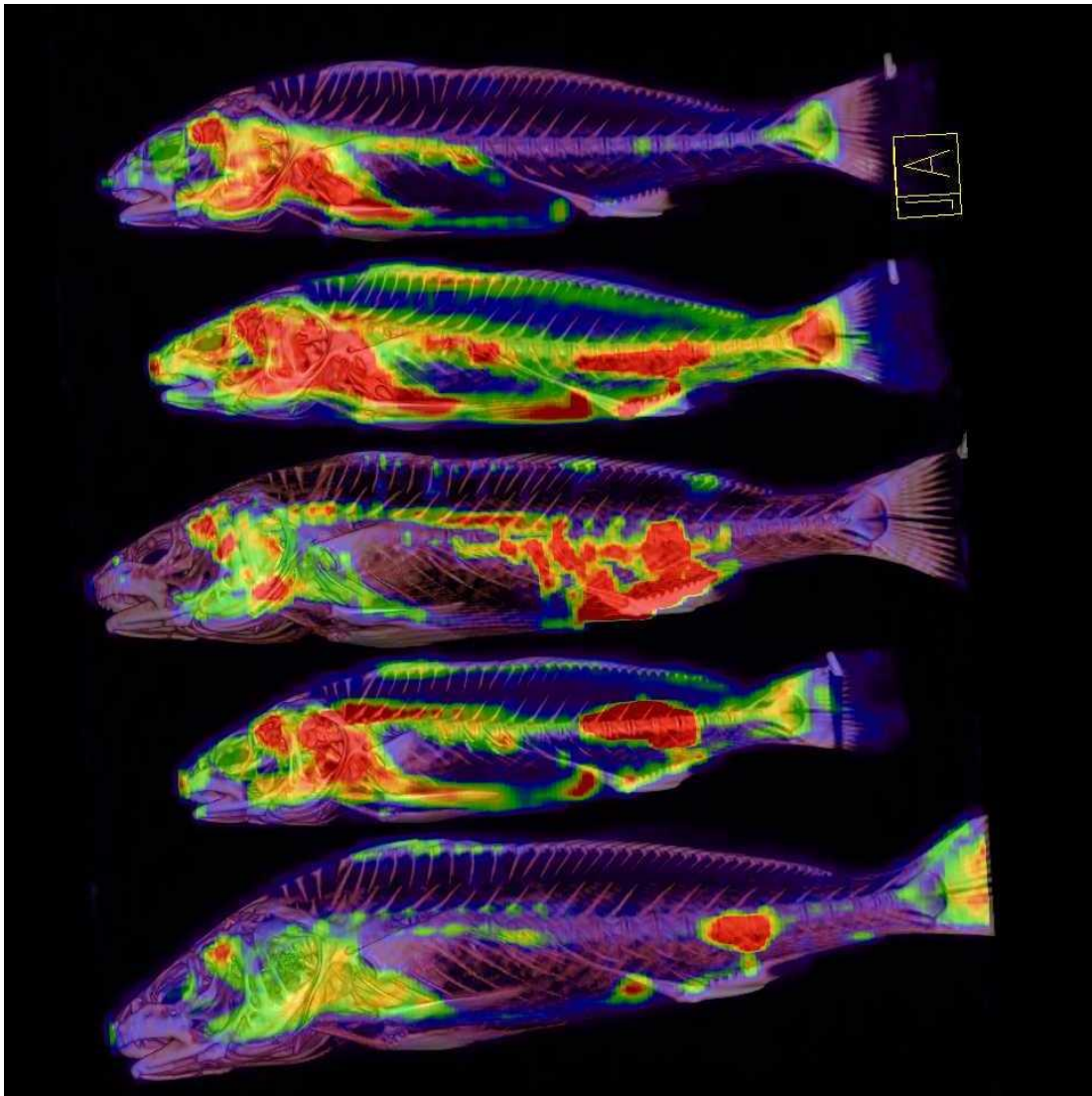


Figure 9: SUV in Each ROI Compared between Fish and Humans. Standard Uptake Values (SUV) of glucose in each ROI compared between fish (n=35) and humans (n=20)18 using the z-test. In all five tissue types, human SUV shows no significant differences as compared to fish ( $p>0.05$ ). Values displayed are mean SUV +/- s.e. Axis labels are the 95% confidence intervals for fish and humans.

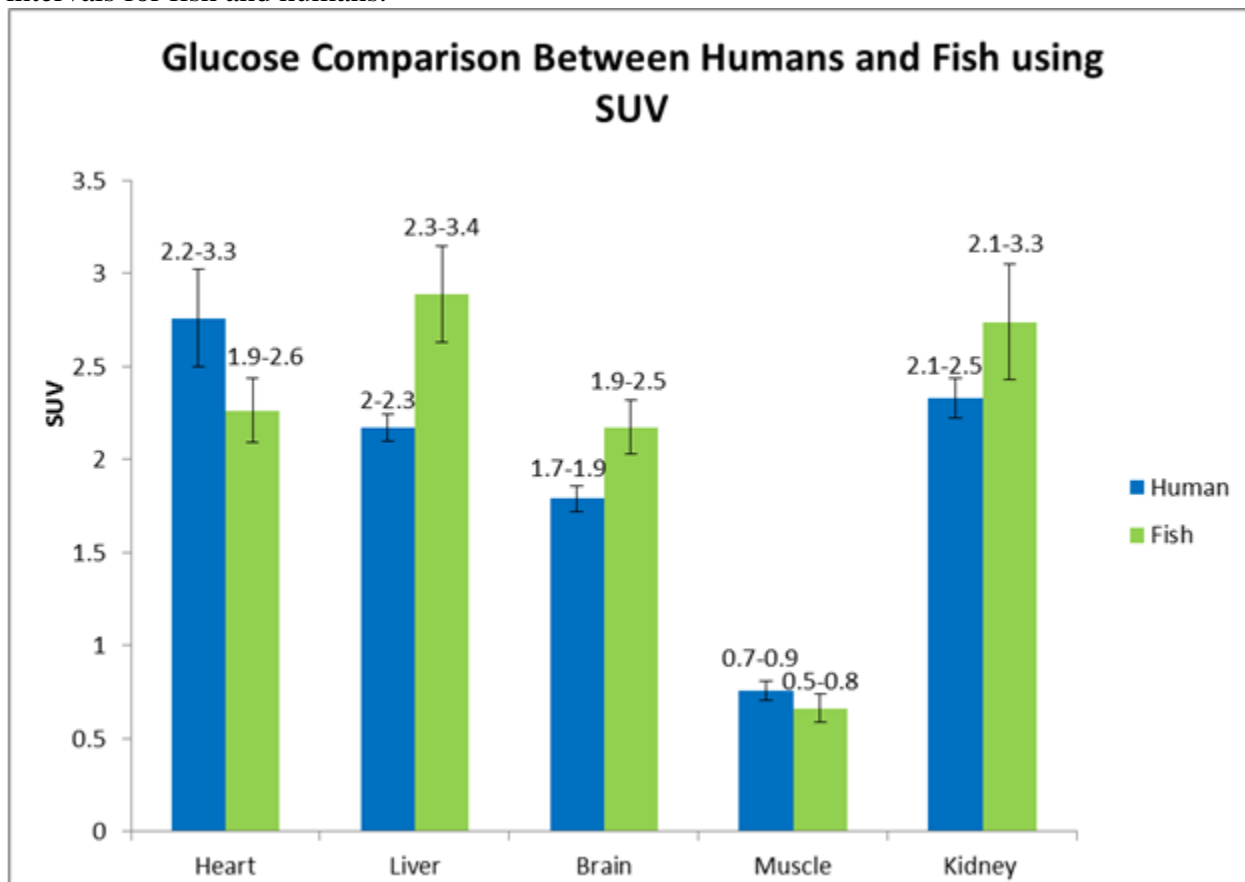


Figure 10: SUV in Each ROI Compared between Fish, Dogs, Mice, and Humans. SUV comparison of glucose in each ROI between dogs (n=7), humans (n=20), mice (n=31), and fish. Each species was compared to humans using the z-test. In all five tissue types, human18 SUV is more similar to fish than mouse22 or dog11 models (p>0.05). Asterisks are used to indicate values that are significantly different from humans (p<0.05). Values displayed are mean SUV +/- s.e.

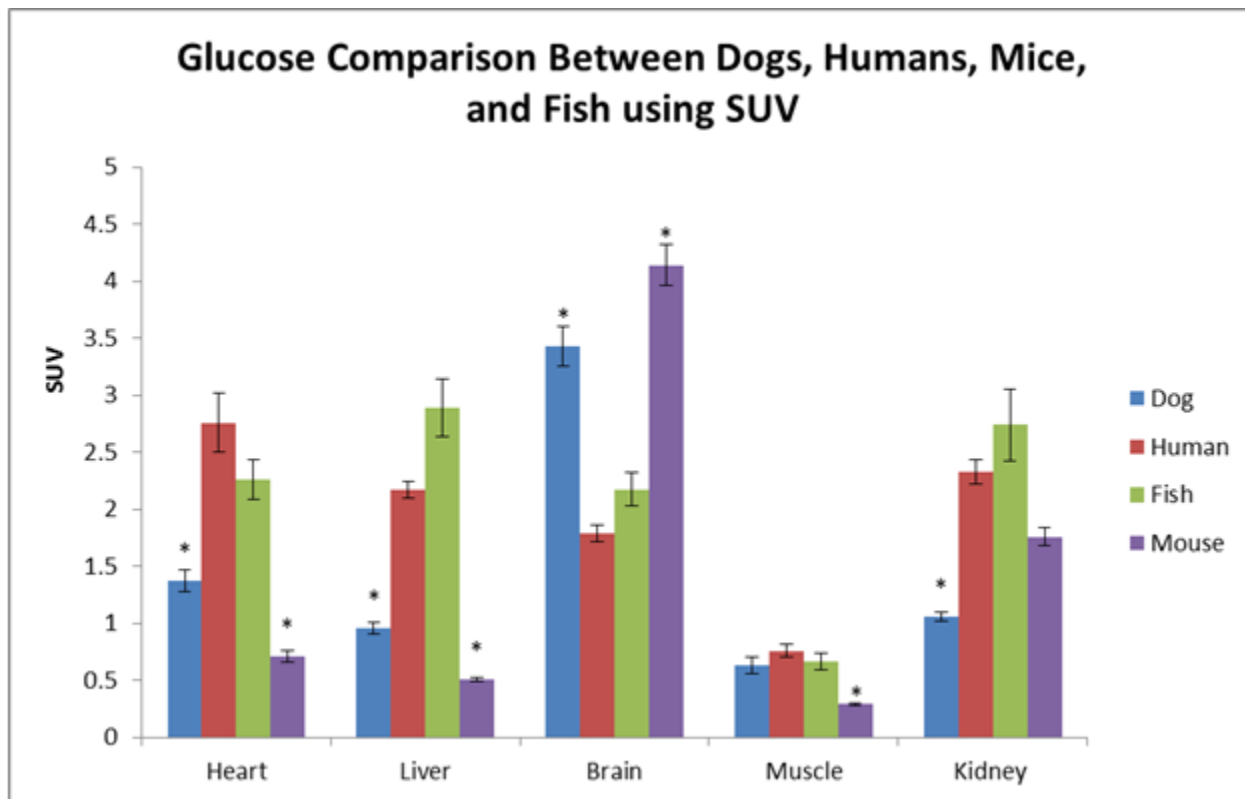


Table 1. Behavioral Measurements. Scoring scale for behavioral measurements of normal and abnormal red drum. Fish were scored daily for 15 d and responses were averaged and compared between the 2 fish groups.

	<i>Score assigned</i>				
<i>Behavior</i>	1	2	3	4	5
<i>Schooling</i>	Fish huddle in tight group with physical contact among multiple fish	Fish are close together but not touching	Fish are dispersed randomly throughout tank	Fish do not associate with one another	Fish actively avoid contact by swimming away from each other
<i>Response to food</i>	Fish scatter quickly when fed	Fish initially swim away from food	Fish do not react	Fish swim closer to food	Fish come to surface and immediately consume food
<i>Response to verbal stimuli</i>	Fish scatter quickly	Fish swim away slowly	Fish do not react	Fish swim closer to speaker	Fish come to surface



Table 2: Summary of Differences between Normal and Abnormal Drum.

<u><i>Response</i></u>	<u><i>Abnormal Drum</i></u>	<u><i>Normal drum</i></u>
<i>Schooling</i>	Low degree of schooling	High degree of schooling
<i>Food</i>	High response to food	Low response to food
<i>Auditory stimuli</i>	Low response to auditory stimuli	High response to auditory stimuli
<i>Cortisol</i>	Higher cortisol	Lower cortisol
<i>Otolith Density</i>	Decreased otolith density	Increased otolith density
<i>Otolith Volume</i>	Increased otolith volume	Decreased otolith volume
<i>Otolith Mass</i>	Equal otolith mass	Equal otolith mass

Table 3: Weight and Lengths of Fish. The lengths in centimeters and the weights in grams for each fish used in the 18 F-Fluorodeoxyglucose PET/CT imaging experiment.

<b><i>Fish Species</i></b>	<b><i>Weight</i></b>	<b><i>Length</i></b>
<i>channel catfish</i>	445	37
<i>channel catfish</i>	431	38
<i>channel catfish</i>	379	35
<i>channel catfish</i>	497	37
<i>channel catfish</i>	323	34
<i>red drum</i>	290	32.5
<i>red drum</i>	358	34
<i>red drum</i>	473	36
<i>red drum</i>	273	30
<i>red drum</i>	574	39.5
<i>grass carp</i>	463	35
<i>grass carp</i>	418	36
<i>grass carp</i>	452	37

Table 3: Continued

<b><i>Fish Species</i></b>	<b><i>Weight</i></b>	<b><i>Length</i></b>
<b><i>grass carp</i></b>	389	37
<b><i>largemouth bass</i></b>	450	33
<b><i>largemouth bass</i></b>	711	39
<b><i>largemouth bass</i></b>	1205	45
<b><i>largemouth bass</i></b>	832	46
<b><i>largemouth bass</i></b>	713	40
<b><i>koi</i></b>	693	34
<b><i>koi</i></b>	980	37
<b><i>koi</i></b>	816	38
<b><i>koi</i></b>	963	38
<b><i>koi</i></b>	901	38
<b><i>hybrid striped bass</i></b>	737	39
<b><i>hybrid striped bass</i></b>	318	30
<b><i>hybrid striped bass</i></b>	1246	47
<b><i>hybrid striped bass</i></b>	1084	50
<b><i>tilapia</i></b>	512	32
<b><i>tilapia</i></b>	514	31
<b><i>tilapia</i></b>	599	32
<b><i>tilapia</i></b>	539	32
<b><i>tilapia</i></b>	648	34

Table 4. 30 Minute SUV of Fish. Means of the Standard Uptake Values (SUV) of fish injected with 18 F-fluorodeoxyglucose (FDG) and imaged 30 minutes post injection. Normal SUV values were measured for the following ROIs for each species of fish (n=5) at 30 minutes post injection: heart, liver, brain, dorsal musculature, and kidney.

<i>Site at 30 Minutes Post Injection</i>	<i>Fish Species N=5</i>	<i>Average SUV <math>\bar{x}</math> (SD)</i>
<b>Heart</b>	Catfish	1.629 (1.269)
	Koi	3.432 (0.833)
	Tilapia	2.682 (0.954)
	Hybrid Striped Bass	3.149 (2.359)
	Large Mouth Bass	1.615 (1.290)
	Red Drum	4.108 (2.153)
	Grass Carp	1.827 (1.199)
<b>Liver</b>	Catfish	1.636 (1.265)
	Koi	4.921 (1.050)
	Tilapia	3.097 (0.809)
	Hybrid Striped Bass	5.976 (3.977)
	Large Mouth Bass	3.193 (0.938)
	Red Drum	3.470 (1.533)
	Grass Carp	1.800 (1.240)
<b>Brain</b>	Catfish	1.145 (1.440)
	Koi	4.320 (0.863)
	Tilapia	2.382 (1.248)
	Hybrid Striped Bass	3.306 (1.746)
	Large Mouth Bass	2.207 (1.152)
	Red Drum	3.205 (1.190)
	Grass Carp	2.115 (1.394)
<b>Muscle</b>	Catfish	0.431 (1.706)
	Koi	0.467 (1.703)
	Tilapia	0.415 (1.711)
	Hybrid Striped Bass	0.769 (1.664)
	Large Mouth Bass	0.456 (1.698)
	Red Drum	0.433 (1.720)
	Grass Carp	0.439 (1.705)
<b>Kidney</b>	Catfish	1.442 (1.363)
	Koi	2.976 (1.169)
	Tilapia	1.618 (1.320)
	Hybrid Striped Bass	6.877 (5.321)
	Large Mouth Bass	3.358 (0.798)
	Red Drum	2.890 (1.768)
	Grass Carp	1.819 (1.240)

Table 5. 60 Minute SUV of Fish. Means of the Standard Uptake Values (SUV) of fish injected with 18 F-fluorodeoxyglucose (FDG) and imaged 60 minutes post injection. Normal SUV values were measured for the following ROIs for each species of fish (n=5) at 60 minutes post injection: heart, liver, brain, dorsal musculature, and kidney. Data for the 60 minute imaging analysis of largemouth bass is unavailable due to a processing error during imaging.

<i>Site at 60 Minutes Post Injection</i>	<i>Fish Species N=5</i>	<i>Average SUV <math>\bar{x}</math> (SD)</i>
<b><i>Heart</i></b>	Catfish	1.426 (1.342)
	Koi	2.740 (0.973)
	Tilapia	2.427 (0.962)
	Hybrid Striped Bass	3.108 (2.408)
	Red Drum	3.616 (1.881)
	Grass Carp	1.348 (1.368)
<b><i>Liver</i></b>	Catfish	1.550 (1.295)
	Koi	4.732 (1.824)
	Tilapia	2.805 (0.849)
	Hybrid Striped Bass	5.464 (2.867)
	Red Drum	3.602 (2.163)
	Grass Carp	1.481 (1.328)
<b><i>Brain</i></b>	Catfish	1.171 (1.430)
	Koi	3.577 (1.120)
	Tilapia	1.872 (1.190)
	Hybrid Striped Bass	3.181 (1.714)
	Red Drum	3.628 (1.937)
	Grass Carp	1.609 (1.331)
<b><i>Muscle</i></b>	Catfish	0.510 (1.679)
	Koi	0.476 (1.708)
	Tilapia	0.368 (1.727)
	Hybrid Striped Bass	0.899 (1.672)
	Red Drum	0.685 (1.637)
	Grass Carp	0.483 (1.688)
<b><i>Kidney</i></b>	Catfish	1.090 (1.464)
	Koi	2.555 (1.199)
	Tilapia	1.191 (1.429)
	Hybrid Striped Bass	5.103 (3.788)
	Red Drum	2.926 (1.829)
	Grass Carp	1.635 (1.298)